

Supplementary material

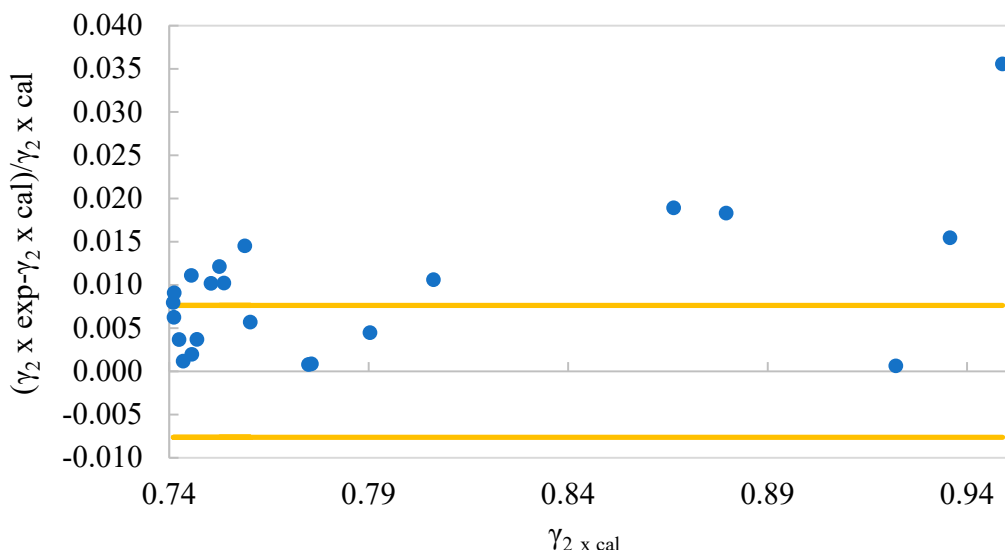


Figure S1. Relative deviation between experimental and calculated values of the activity coefficient at 298.15K from the data of [1]. The horizontal lines correspond to the average relative deviations of the fit.

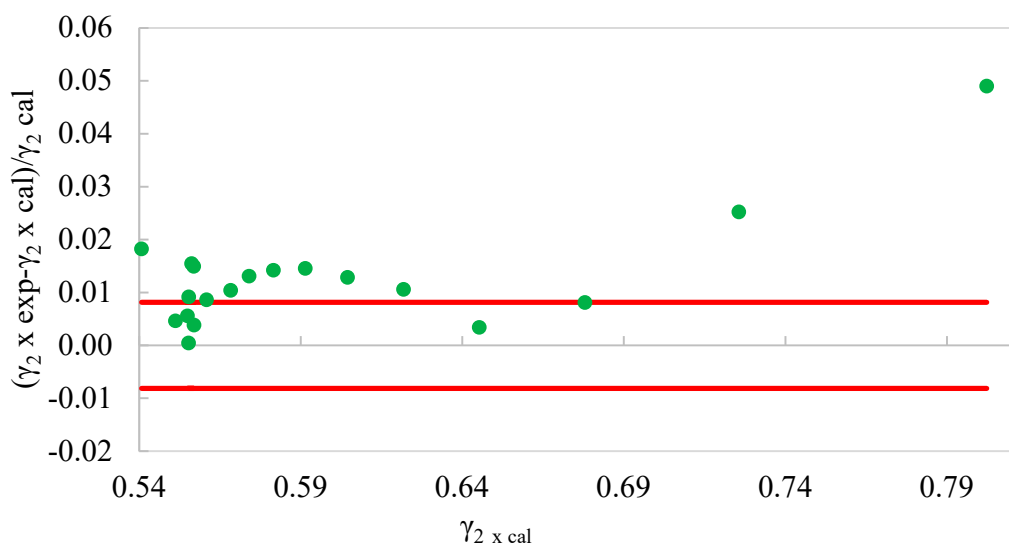


Figure S2. Relative deviation between experimental and calculated values of the activity coefficient at 298.15°K from the data of [27]. The horizontal lines correspond to the average relative deviations of the fit.

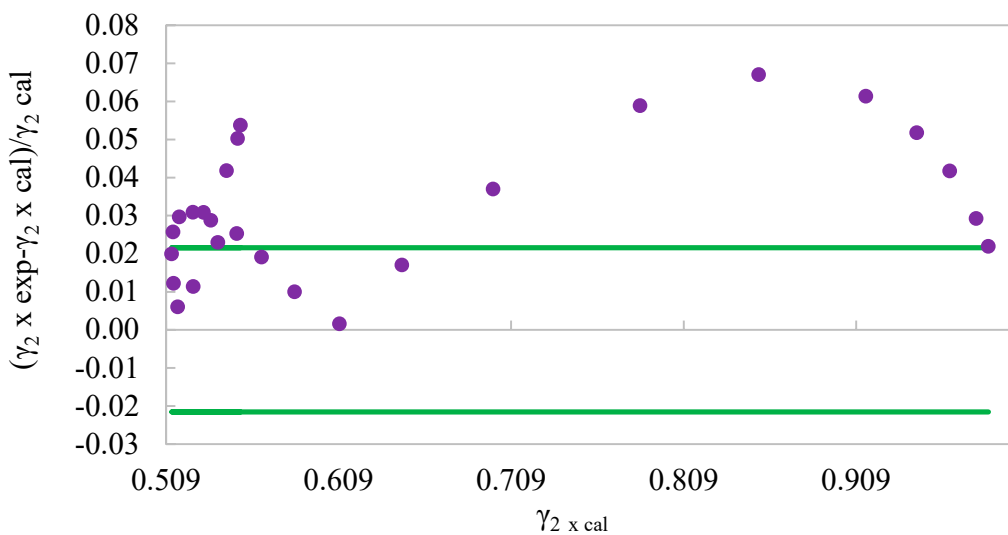


Figure S3. Relative deviation between experimental and calculated values of the activity coefficient at 298.15°K from the data of [28]. The horizontal lines correspond to the average relative deviations of the fit.

Table S1. Density and dielectric constant data of ethanol at different temperatures

T/K	ρ (kg/m ³)	T/K	D
288.15	0.7936	293.15	25
298.15	0.7851	298.15	24.2
308.15	0.7764	303.15	23.55
318.15	0.7676	313.15	22.2
328.15	0.7586	323.15	20.87

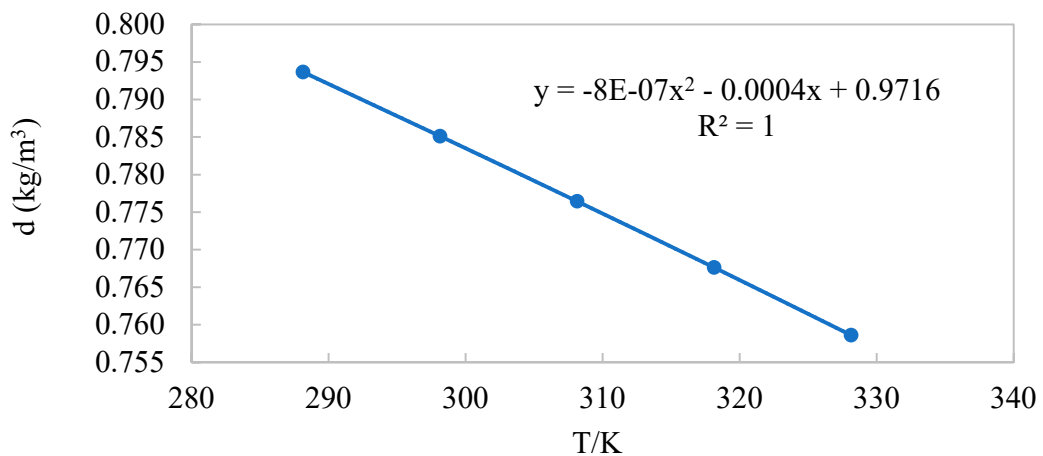


Figure S4. Density at different temperatures.

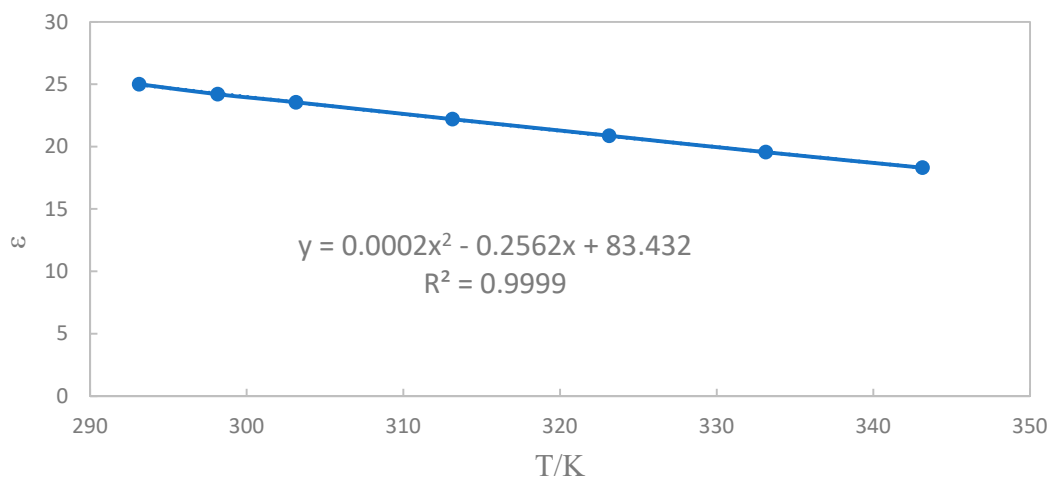


Figure S5. Dielectric constant at different temperatures.

Table S2. Solubility product, K_{ps}, initial solubility, X₀, water activity, a, amount of CHLiO₂ precipitate in mole fraction and g/kg solv, as a function of ethanol weight percentage, and yield (Y) of the process at 283.15 K.

K_{ps}	X_0	a	Ppt (frac. Mol)	Ppt (g/kg solv)	W% Ethanol	Y
0.0225	0.1123	0.7631	0	0.0004	0	0.00
		0.7099	0.0147	59.4903	10.11	5.95
		0.6536	0.0195	73.1100	20.12	7.31
		0.6348	0.0266	91.1184	30.43	9.11
		0.5957	0.0326	102.3803	40.47	10.24
		0.5597	0.0305	86.0589	51.72	8.61
		0.5429	0.0317	80.9148	61.19	8.09
		0.4281	0.0263	59.4085	71.63	5.94
		0.0186	0.0010	2.1035	81.35	0.21

Table S3. Solubility product, Kps, initial solubility, X_0 , water activity, a, amount of CHLiO₂ precipitate in mole fraction and g/kg solv, as a function of ethanol weight percentage, and yield (Y) of the process at 293.15 K.

K_{ps}	X_0	a	Ppt (frac. Mol)	Ppt (g/kg solv)	W% Ethanol	Y
0.0197	0.1206	0.7563	0	0.1961	0	0.02
		0.6987	0.0172	70.5595	10.29	7.06
		0.6596	0.0274	102.3469	21.76	10.23
		0.6268	0.0294	101.8818	30.52	10.19
		0.6026	0.0338	106.8965	40.53	10.69
		0.6010	0.0347	99.4729	50.76	9.95
		0.5961	0.0365	94.2690	60.70	9.43
		0.3786	0.0245	55.7608	71.6	5.58
		0.0060	0.0004	0.8364	81.29	0.08

Table S4. Solubility product, Kps, initial solubility, X_0 , water activity, a, amount of CHLiO₂ precipitate in mole fraction and g/kg solv, as a function of ethanol weight percentage, and yield (Y) of the process at 298.15 K.

K_{ps}	X_0	a	Ppt (frac. Mol)	Ppt (g/kg solv)	W% Ethanol	Y
0.0184	0.1250	0.7533	0.0000	0.1093	0.00	0.01

0.6977	0.0189	77.6651	10.00	7.77
0.6396	0.0234	89.0865	20.24	8.91
0.5973	0.0284	99.1599	30.28	9.92
0.5509	0.0305	96.9808	40.60	9.70
0.5359	0.0312	89.5217	51.22	8.95
0.4901	0.0320	82.7153	60.90	8.27
0.3775	0.0254	57.8121	71.70	5.78
0.0169	0.0011	2.2578	81.64	0.23

Table S5. Solubility product, Kps, initial solubility, X_0 , water activity, a , amount of CHLiO₂ precipitate in mole fraction and g/kg solv, as a function of ethanol weight percentage, and yield (Y) of the process at 303.15 K.

K _{ps}	X ₀	a	Ppt (frac. Mol)	Ppt (g/kg solv)	W% Ethanol	Y
0.0172	0.1313	0.7423	0.0000	0.1994	0.00	0.02
		0.6839	0.0196	80.9690	10.40	8.10
		0.6306	0.0268	101.4063	21.30	10.14
		0.5693	0.0326	112.8889	32.20	11.29
		0.5305	0.0342	105.9216	44.10	10.59
		0.4780	0.0317	87.8416	55.20	8.78
		0.4328	0.0292	73.4293	63.80	7.34
		0.2310	0.0158	34.8422	74.70	3.48
		0.0000	0.0000	0.0113	85.60	0.00

Table S6. Solubility product, Kps, initial solubility, X_0 , water activity, a , amount of CHLiO₂ precipitate in mole fraction and g/kg solv, as a function of ethanol weight percentage, and yield (Y) of the process at 313.15 K.

K _{ps}	X ₀	a	Ppt (frac. Mol)	Ppt (g/kg solv)	W% Etanol	Y
0.0150	0.1443	0.7212	0.0000	0.2046	0.00	0.02

0.6683	0.0200	84.2138	10.00	8.42
0.6163	0.0276	106.5906	21.00	10.66
0.5716	0.0312	110.6054	31.00	11.06
0.5274	0.0360	114.6035	42.70	11.46
0.5285	0.0388	112.2846	51.80	11.23
0.5131	0.0373	96.7585	61.70	9.68
0.4135	0.0320	73.6483	71.60	7.36
0.0171	0.0013	2.5248	81.90	0.25

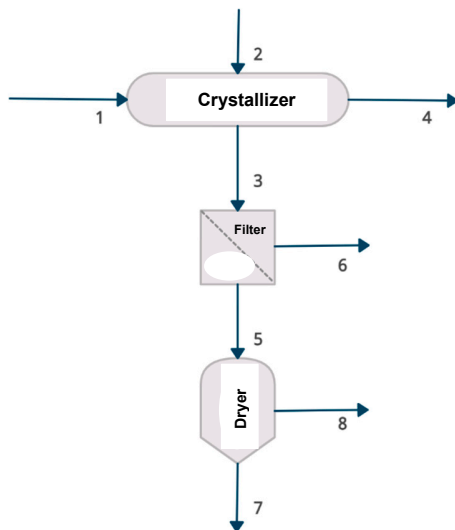


Figure S6. Drowning-out crystallization process of LiOH at 298.15 K

Mathematical definition of the terms of Equations (10)-(12) in section 2.2

$$m_i = \frac{n_i}{n_w} ; (i = 1, 2) \quad \text{Equation (S1)}$$

$$B_{11} = \lambda_{11} \quad \text{Equation (S2)}$$

$$C_{111} = \mu_{111} \quad \text{Equation (S3)}$$

$$B_{22} = \lambda_{ca} + \frac{v_c}{2v_a}\lambda_{cc} + \frac{v_a}{2v_c}\lambda_{aa} \quad \text{Equation (S4)}$$

$$C_{222}^\phi = \frac{3}{(v_a v_c)^{\frac{1}{2}}} (\mu_{ca} + \mu_{aa} v_a) \quad \text{Equation (S5)}$$

$$C_{222}^{\gamma} = \frac{3}{2} C_{222}^{\phi} \quad \text{Equation (S6)}$$

$$B_{12} = 2(\lambda_{1c} v_c + \lambda_{1a} v_a + \mu_{11a} v_a) \quad \text{Equation (S7)}$$

$$C_{112} = 3(\mu_{11c} v_c + \mu_{11a} v_a) \quad \text{Equation (S8)}$$

$$C_{122} = 3(\mu_{1cc} v_c^2 + 2\mu_{1ca} v_c v_a + \mu_{1aa} v_a^2) \quad \text{Equation (S9)}$$

The expressions B'_{12} and B'_{22} are the derivatives of B_{12} and B_{22} with respect to I , respectively. Using the same method as in the original Pitzer model this for univalent salts, the second global virial coefficients can be calculated with Eq. (22), where: $\beta^{(0)}$, $\beta^{(1)}$ and α possess similarity to those of the original Pitzer's viral model.

$$B_{ij} = \beta_{ij}^{(0)} + \frac{2\beta_{ij}^{(1)}}{\alpha_{1,ij}^2 I} \left[1 - \left(1 + \alpha_{1,ij} I^{\frac{1}{2}} \right) \exp \left(-\alpha_{1,ij} I^{\frac{1}{2}} \right) \right] \quad \text{Equation (S10)}$$

Correlation of vapor-liquid equilibrium (VLE) data of ternary systems shows that it is not sensitive to the parameter α , and any value of α selected close to that given by Pitzer is possible to use. Therefore, values of $\alpha_{1,12} = \alpha_{1,22} = 2.0$ are used.